Development 133, 4805-4813 (2006) doi:10.1242/dev.02689

Threshold response of *C15* to the Dpp gradient in *Drosophila* is established by the cumulative effect of Smad and Zen activators and negative cues

Meng-chi Lin, Jeongsook Park, Nikolai Kirov and Christine Rushlow*

Morphogen gradients determine a range of cell fates by specifying multiple transcriptional threshold responses. In the dorsal ectoderm of the *Drosophila* embryo, a BMP gradient is translated into an activated Smad transcription factor gradient, which elicits at least three threshold responses – high, intermediate and low. However, the mechanism underlying differential response to Dpp is poorly understood, due in part to the insufficient number of well-studied target genes. We analyzed the regulation of the *C15* gene, which can be activated in cells containing intermediate levels of Dpp. We show that *C15* expression requires both *dpp* and *zen*, thus forming a genetic feed-forward loop. The *C15* regulatory element contains clusters of Smad- and Zen-binding sites in close proximity. Mutational analysis shows that the number of intact Smad- and Zen-binding sites is essential for the *C15* transcriptional response, and that the spatial limits of *C15* expression are established through a repression mechanism in the dorsolateral cells of the embryo. Thus, the combinatorial action of Smad and Zen activators bound to a number of adjacent sites, and competing negative cues allows for proper gene response to lower than peak levels of the Dpp morphogen.

KEY WORDS: Dpp target gene, Dpp gradient, Zen, Feed-forward, *Drosophila*

INTRODUCTION

Morphogens are key regulatory molecules that determine multiple cell fates in a concentration-dependent manner across a field of cells (reviewed by Gurdon and Bourillot, 2001; Ashe and Briscoe, 2006). A particular level of morphogen acts to elicit a specific expression profile that eventually leads to a specific cell behavior. Many signaling molecules have been shown to act as morphogens, including members of the Hedgehog, Wingless and TGFβ families of secreted molecules (reviewed by Gurdon and Bourillot, 2001). For example, gradients of Bone morphogenetic proteins (Bmps) act in *Xenopus* (Wilson et al., 1997) and *Drosophila* embryonic ectoderm patterning (Ferguson and Anderson, 1992; Wharton et al., 1993) and *Drosophila* adult wing formation (Lecuit et al., 1996; Nellen et al., 1996). How these gradients are interpreted by receiving cells is not fully understood. The simplest mechanism is a direct readout of the gradient after its conversion into a gradient of intracellular transcription factors (Wilson et al., 1997). This has been demonstrated in the *Drosophila* embryo for the Bmp ligand Decapentaplegic (Dpp) and its transducing transcription factor, phosphorylated Mad (Mad-*P*). The graded distribution of Mad-*P* (Dorfman and Shilo, 2001; Rushlow et al., 2001; Sutherland et al., 2003) is very similar to that of receptor-bound Dpp (Shimmi et al., 2005; Wang and Ferguson, 2005). Early in cellular blastoderm formation, receptor-bound Dpp and Mad-*P* are distributed at low levels in a broad dorsally localized domain, but soon a steep stepwise gradient emerges. By the end of cellularization, high levels are present in a five- to six-cell-wide strip of cells along the dorsal midline, while lower levels are detected in three to four cells to either side of the strip.

Department of Biology, New York University, 100 Washington Square East, New York, NY 10003, USA.

*Author for correspondence (e-mail: chris.rushlow@nyu.edu)

Accepted 10 October 2006

Cells respond to different levels of Mad-*P* by activating target genes in nested domains that correlate with different concentrations of the Dpp/Mad-*P* gradient (reviewed by Ashe and Briscoe, 2006). For example, *Race* (*Ance* – Flybase) (Tatei et al., 1995) and *hindsight* (*hnt*) [*pebbled* (*peb*) – Flybase] (Ashe et al., 2000) are activated in the region of high-level Mad-*P*. They define the highest threshold of the Mad-*P* gradient and are referred to as Threshold Type I genes (Ashe et al., 2000). *u-shaped* (*ush*) (Jazwinska et al., 1999) and *tailup* (*tup*) (Ashe et al., 2000) are expressed in a broader domain of 12 to 14 cells comprising high and lower levels of Mad-*P* and are referred to as Type II genes. *pannier* (*pnr*) extends more laterally into the region in which Mad-*P* is undetectable by current techniques, encompassing a domain of 36 to 40 cells (Jazwinska et al., 1999), and represents the Type III genes.

By what mechanism do these target genes respond differentially to the Mad-*P* gradient? The classic paradigm of how threshold responses are determined was established years ago from studies on the *Drosophila* morphogens Bicoid (Driever et al., 1989) and Dorsal (Jiang and Levine, 1993), and is based on the relative affinities of morphogen-binding sites in target-gene enhancers. Target genes activated in regions in which low concentrations of morphogen are present contain high-affinity binding sites in their enhancers. Targets activated in regions of high-level morphogen contain low-affinity binding sites, but if those sites are changed to high-affinity sites, activation can now occur in regions of low-level morphogen (Driever et al., 1989; Jiang and Levine, 1993). Although this mechanism has been established for some Dorsal and Bicoid targets, it may not be sufficient to explain the differential regulation of all their targets, or of Dpp targets. In fact, a recent study on several Bicoid target genes using bioinformatics tools suggested that the affinity model is insufficient to explain how threshold borders are determined (Ochoa-Espinosa et al., 2005).

Studies on the Dpp target *Race* demonstrated that in addition to the relative-affinity mechanism, a combinatorial mechanism of interacting activators is involved in establishing transcription limits of Dpp targets. Support for the relative-affinity model comes from

a study by Wharton et al. (Wharton et al., 2004). The *Race* enhancer contains several Smad sites, one of which has a relatively high affinity to Smads compared with the others. When two low-affinity sites were changed into higher affinity sites in a *Race-lacZ* reporter gene, the expression border expanded into regions containing low levels of Mad-*P*. However, Xu et al. (Xu et al., 2005) showed that a combinatorial mechanism is also utilized in which Dpp, via the Smads, and Zerknüllt (Zen), a homeodomain protein (Doyle et al., 1986), act together to activate *Race*. Zen-binding sites lie in close proximity to Smad sites in the enhancer, and both types of sites are required for normal activation of the *Race-lacZ* reporter (Xu et al., 2005). Furthermore, as Zen itself is a target gene of high-level Dpp in the late blastoderm stage (Rushlow et al., 2001), *Race* regulation represents a feed-forward regulatory circuit, in which one regulator, Dpp, activates a second regulator, Zen, and then both activate a common target gene, *Race*. It was proposed that all Type I Dpp targets are regulated in a similar way (Xu et al., 2005).

Here we investigate the mechanism by which the Dpp target gene *C15* is regulated. *C15* is expressed along the dorsal midline in a five- to ten-cell-wide stripe, the lateral border of which lies within the region of intermediate-level Mad-*P*. Surprisingly, we found that the relative affinity of Smad-binding sites in the *C15* enhancer does not play a major role in establishing this domain. Instead, combinatorial regulation involving Smad/Zen feed-forward circuitry, the relative numbers of Smad- and Zen-binding sites, and a repression mechanism is important for the *C15* pattern of expression.

MATERIALS AND METHODS

Fly strains

dpp^{hr4} is a weak hypomorphic allele balanced over *SM6 eve-lacZ* and dpp^{H46} is a null allele balanced over *CyO23, P[dpp+]* (Wharton et al., 1993). sog^{YS06} is a null allele of *sog* (Francois et al., 1994) balanced over *FM7c, ftz-lacZ*. zen^{w36} is a null allele (Rushlow et al., 1987) balanced over *TM3, ftz-lacZ*. The double heterozygous embryos, dpp^{hr4}/+; zen^{w36}/+, were identified by the lack of *lacZ* staining in embryos derived from a cross of the dpp^{hr4} and zen^{w36} stocks. To obtain uniform early embryonic expression of *UAS-zen*, a maternal *GAL4* driver was used where a *GAL4-VP16* fusion protein is expressed under the control of the *α-tubulin 67C* promoter.

Bacterial expression of Zen, Mad and Medea

The GST-Zen expression plasmid contains the full-length *zen* coding region (Xu et al., 2005). GST-Mad^N (Kim et al., 1997) and GST-Medea (Xu et al., 1998) fusion proteins contain the N-terminal MH1 domains. The expression and the purification of the recombinant proteins were carried out as described before (Rushlow et al., 2001).

In vitro mutagenesis and transgenic analysis

DNA fragments summarized in Fig. 2 were prepared by PCR using genomic DNA as template (Clontech) and the Expand High Fidelity PCR System (Roche Biochemicals). Amplified fragments were first cloned into the pCRII vector using the TOPO cloning system (Invitrogen) and then subcloned into the p*CasPeRhs43-βgal* transformation vector to make transgenic flies. The mutagenesis of Zen- and Mad-binding sites was performed using the PCR method with the same mutated oligonucleotides used in the mobility shift assays (see Figs 3 and 4 for sequences).

In vitro DNA-binding assays

DNAse I footprint analyses and electrophoretic mobility shift assays were carried out as previously described (Kirov et al., 1993). For Zen footprinting assays, five fragments were generated from the 650-3 bp *C15* enhancer fragment using convenient restriction sites: I (1-63 bp), II (59-459 bp), III (59-311 bp), IV (310-652 bp) and V (457-652 bp). For the Smad mobility shift assays, 14 fragments were isolated: A (1-127 bp), B (124-311 bp), C (310-459 bp), D (457-516 bp), E (517-588 bp), F (585-652 bp), G (1-60 bp), H (82-156 bp), I (169-256 bp), J (257-299 bp), K (59-156 bp), L (154-237 bp), M (300-397 bp), N (387-459 bp). The sequences of the wild-type and mutant oligonucleotides spanning the putative Zen- and Smad-binding sites are listed in Figs 3 and 4.

In situ hybridization and antibody staining

Wild-type, mutant and transgenic embryos were fixed, hybridized with *C15* and/or *lacZ* (to detect transgenes expressed from balancer chromosomes or to detect the *lacZ* transgene activity) antisense RNA probes, stained (Roche Molecular Biochemicals), and mounted in araldite (Polysciences) or Aquamount (Polysciences) as previously described (Rushlow et al., 2001). Wild-type embryos were stained with anti-phospo-Smad1 antibodies as previously described (Rushlow et al., 2001).

RESULTS

C15 is a homeobox gene first identified as a member of the 93DE homeobox cluster located on chromosome 3R that includes *NK4/tinman* (*tin*), *NK3/bagpipe* (*bap*), *ladybird late* (*lbl*), *ladybird early* (*lbe*), *C15* and *NK1/slouch* (*slou*) in the proximal-to-distal order (Dessain and McGinnis, 1993; Jagla et al., 2001). All but *C15* have been shown to be required for mesoderm tissue specification (Jagla et al., 2001). *C15* mutant flies have appendage phenotypes, including lack of the tarsal claws (Campbell, 2005; Kojima et al., 2005), hence *C15* is also called *clawless* (*cll*) (Koijma et al., 2005). No embryonic phenotypes have been described for *C15* mutants, although *C15* is expressed throughout embryogenesis (Dear and Rabbitts, 1994).

C15 is initially expressed during stage 5 in a stripe along the dorsal midline (Fig. 1A) (Stathopoulos et al., 2002). The width of the stripe varies from five to ten cells (Fig. 1A, inset); thus, at its widest, *C15* creeps into the region in which cells contain low levels of Mad-*P* (Fig. 1B). *C15* is wider than *Race* (a Type I target; Fig. 1C), but not as broad as *tup* (a Type II target; Fig. 1D). The variability in *C15* expression along the anteroposterior (AP) axis is not atypical for dorsally expressed genes (Fig. 1A,C,D). *C15* continues to be expressed in the dorsal region throughout gastrulation, and can be observed in the differentiated amnioserosa and a few rows of dorsolateral cells in older embryos (data not shown).

C15 is regulated by a Smad/Zen feed-forward loop

In order to better characterize the threshold response to Dpp of C15, we examined its expression in *dpp*, *zen* and *sog* mutant backgrounds, as well as in a situation in which Zen is overexpressed throughout the embryo. Like the Type I gene *Race* (Xu et al., 2005), *C15* is absent in dpp^{hr4} hypomorphic (Fig. 1E) and dpp^{H46} amorphic mutants (data not shown), zen^{w36} amorphs (Fig. 1F), and in the double heterozygote (dpp^{hr4}/+, zen^{w36}/+; data not shown), although *C15* is normal in the single heterozygotes (dpp^{hr4}/+ and zen^{w36}/+; data not shown). The levels of Mad-*P* and *zen* in the *dpp* mutant backgrounds have been reported (Rushlow et al., 2001). In dpp^{hr4} Mad-*P* is present at a very low level, while *zen* is at a medium level in a broad domain that never refines. In dpp^{H46} mutants, Mad-*P* is absent and *zen* disappears in early stage 5. In *zen* mutants, Mad-*P* is mostly normal, although the peak levels of Mad-*P* are slightly diminished (Wang and Ferguson, 2005) (C.R., unpublished). These results indicate that, like *Race*, *C15* requires relatively high levels of both Dpp and Zen (Xu et al., 2005).

By contrast, *C15* behaved differently from *Race* in *sog* mutants. *C15* is strongly expressed in a broad dorsal domain comprising the middle body region (Fig. 1G), whereas *Race* expression is spotty at best (Ashe et al., 2000; Xu et al., 2005). Mad-*P* does not form a gradient in *sog* mutants and never reaches peak levels, but instead remains at a medium level throughout the dorsal half of the embryo

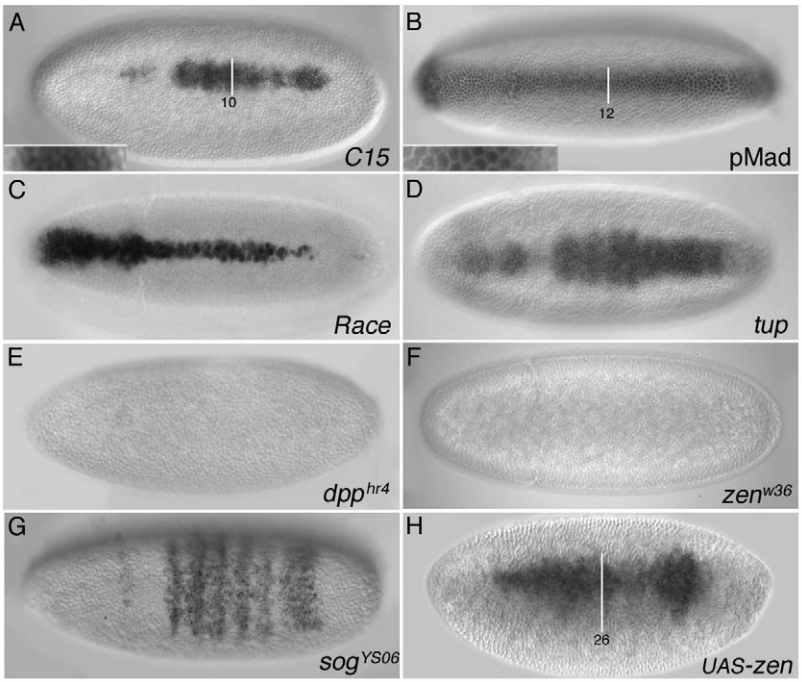

Fig. 1. The threshold response of *C15* to the Mad-*P* gradient depends on both Smads and Zen. Dorsal views of late stage 5/early stage 6 embryos with anterior to the left. The widest area of expression is delineated with a white line labelled to show the width in number of cells. (**A**) Wild-type embryo hybridized with *C15* probes. Transcripts are present in a five- to ten-cell-wide dorsal strip of cells in the main body region and a faint spot in the presumptive head region. Cells in this region are magnified in the inset, which lies perpendicular to the embryo. (**B**) Wild-type embryo stained with an anti-phospho-Smad1 antibody, which also recognizes Mad-*P*. Strong staining is observed in a five- to six-cell-wide stripe with less staining in three to four cells to either side of the stripe (see magnified inset). In terminal regions, the Mad-*P* stripe can be up to 16 cells wide. (**C**) Wild-type embryo hybridized with *Race* probes. Transcripts are present in a four- to six-cell-wide stripe. (**D**) Wild-type embryo hybridized with *tup* probes. The dorsal stripe is ten to 14 cells wide. (**E**-**H**) Mutant embryos hybridized with *C15* probes. *C15* is absent in *dpp*^{hr4} homozygotes (E) and *zen*^{w36} homozygotes (F). *C15* is in a broad domain in *sog*^{YS06} hemizygous embryos (G). The *C15* pattern broadens to about 26 cells at its widest in a *maternal GAL4>UAS-zen* embryo (H).

where *C15* expression is observed (Rushlow et al., 2001; Raftery and Sutherland, 2003). In addition, the *zen* pattern does not refine into a strong dorsal stripe but also remains broad and at medium levels (Rushlow et al., 2001). These levels of Mad-*P* and Zen cannot activate *Race* (Xu et al., 2005), but are nevertheless sufficient to activate *C15* (Fig. 1G). Thus we conclude that *C15* resembles Type II genes because it requires less Mad-*P* than the Type I genes for transcriptional activation.

As *C15* is absent in *zen* mutants, it is possible that *C15* expression does not depend on Mad-*P* directly, but rather Mad-*P* activates *zen*, and then Zen activates *C15*. *zen* refinement to the dorsalmost five to six cells is dependent on high levels of Mad-*P* (Rushlow et al., 2001), and although *zen* RNAs are restricted to this domain, Zen protein is detectable in a few cells lateral to the five- to six-cell-wide stripe, but at lower levels (Rushlow et al., 1987). This low-level Zen could provide a critical input for the activation of *C15*. We assayed embryos in which *zen* is expressed ubiquitously. We previously reported that the Mad-*P* gradient was not affected in such a situation (Xu et al., 2005). Embryos carrying *UAS-zen* and a maternal-*GAL4* driver showed a broadened *C15* pattern, encompassing about 26 cells at its widest point (Fig. 1H). This domain is not as wide as *pnr* (32-36 cells), but it is much wider than *tup* (12-14 cells). Thus, Zen is able to activate *C15* ectopically; however, this requires some specific level of Mad-*P*, which in the absence of zen is not adequate. Our genetic results support the idea that *C15* is regulated by the combined activity of Smads and Zen in a feed-forward loop.

A 650 bp enhancer in the *C15* second intron drives early blastoderm expression

To study the possibility that both Smads and Zen bind to the *C15* regulatory region, we first searched for an enhancer that mediates *C15* blastoderm expression. Overlapping DNA fragments comprising the 30 kb region that includes *C15* and its immediately adjacent genes were tested in transgenic reporter gene assays for early embryonic expression by in situ hybridization with *lacZ* RNA probes. The fragment containing the second intron (I-2) was able to drive *lacZ* expression in a *C15*-like dorsal stripe pattern (Fig. 2B).

The I-2 fragment was divided into five smaller overlapping fragments and subjected to the same analysis (results are summarized in Fig. 2A; blue lines denote *lacZ* expression). Two fragments, I-2-4 and I-2-5, were able to drive blastoderm expression. *I-2-5-lacZ* embryos showed a *C15*-like dorsal stripe (data not shown), however, *I-2-4-lacZ* embryos showed a broader than normal dorsal stripe, especially in the middle body region (Fig. 2C), implying that the I-2-4 fragment is missing a negative regulatory element that is present in the I-2 and I-2-5 fragments.

To further delineate the early enhancer, several smaller constructs were tested (Fig. 2A). Of these, only the 650-3 (650 bp in length) and the 350-2 (about 350 bp and included within the 650-3) fragments were able to drive a *lacZ* pattern similar to the endogenous *C15* pattern (Fig. 2D,E, respectively), although the *350-2-lacZ* pattern was weaker in intensity. Both of these constructs contain sequences from I-2-5 that are not present in I-2-4, and thus harbor the putative negative element in I-2-5. Importantly, both the *650-3-lacZ* and the smaller *350-2-lacZ* were able to drive a *C15*-like dorsal stripe. Furthermore, when crossed into a *sog* mutant background, this pattern broadened (data not shown) like endogenous *C15* in a *sog* mutant. These results confirm that the minimal sequences necessary for the qualitative *C15* response to the Mad-*P* gradient is contained within the 350 bp minimal enhancer fragment. However, for a full quantitative response, additional sequences present in the full 650 bp enhancer are necessary.

The *C15* enhancer contains multiple Zen and Smad sites

We used in vitro DNA-binding assays to search for Zen- and Smad-binding sites in the 650 bp *C15* enhancer. To identify Zen-binding sites, we performed DNAse I protection (footprinting) assays with five overlapping DNA fragments that span the 650 bp enhancer region and recombinant GST fused Zen (GST-Zen) protein (Fig. 3A). Protection was observed at two distinct regions in fragment IV, which we designated Z1 and Z2, and at one region in fragment V, Z3 (Fig. 3B and C). The Z1 and Z3 sites contain an ATTA homeodomain core recognition sequence (Kissinger et al., 1990),

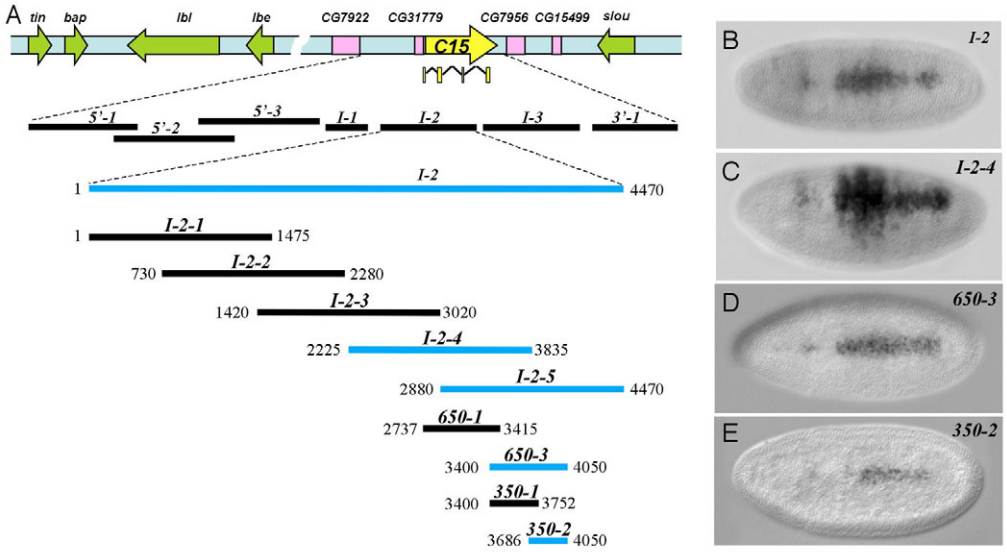

Fig. 2. A 650 bp enhancer is sufficient to drive the *C15* dorsal-stripe pattern. (**A**) The *C15* gene (yellow arrow) is located in the 93DE homeobox gene cluster (green arrows) (Jagla et al., 2001), which also contains predicted genes (pink boxes). Several overlapping DNA fragments comprising approximately 30 kb of 5′, 3′ and intronic (I) DNA of the *C15* gene were tested in *lacZ* reporter assays, some of which were capable of activating *lacZ* expression in blastoderm embryos (blue lines). (**B**-**E**) Embryos hybridized with *lacZ* probes. (B) *I-2-lacZ* shows a *lacZ* pattern identical to the endogenous *C15* pattern. (C) *I-2-4-lacZ* shows a broader pattern, suggesting that a negative element is missing. (D) *650-3* shows a *lacZ* pattern like that of I-2. (E) *350-2* shows weaker *lacZ* expression than the *650-3*.

and Z2 contains an AT-rich sequence, A**AATTGATT**T, that is similar to the AT-rich homeodomain-binding consensus sequence, TCAATTAAAT (Desplan et al., 1988; Hoey and Levine, 1988). Z3 also contains an AT-rich sequence **AATTTATT**GTT (reverse strand from footprint) that is very similar to the one in Z2 (identical for the seven nucleotides in bold type). Gel shift assays with oligonucleotides spanning the AT-rich sequences in Z1, Z2 and Z3 (Fig. 3E, putative Zen-binding sites in red) and oligonucleotides with mutations in the AT-rich sequences ($Z1^m$, $Z2^m$, $Z3^m$; mutated nucleotides in green) further confirmed the specific binding of Zen to these AT-rich sequences. Strong binding was observed with the wild-type oligonucleotides (Fig. 3D, lanes 2, 6 and 10), but binding was dramatically reduced when the AT-rich sequences were mutated (Fig. 3D, lanes 4, 8 and 12). Therefore the AT sequences in Z1, Z2 and Z3 (two sites) represent the Zen-binding sites in the *C15* enhancer. All of these Zen-binding sites are contained in the 350-2 *C15* minimal enhancer.

In order to determine the Smad-binding sites in the *C15* enhancer, mobility shift assays were performed with overlapping enhancer fragments that span the 650 bp enhancer region (schematized in Fig. 4A) and recombinant GST-fused Mad (GST-Mad) and GST-fused Medea (GST-Med) proteins (Kim et al., 1997; Xu et al., 1998). The results are summarized in Fig. 4A (bound fragments are denoted in blue; gels are not shown). Mad and Medea were able to bind the same fragments, although with slightly different intensities (data not shown).

To identify the specific sequences responsible for Smad binding, we searched the DNA sequence of the bound fragments for the presence of GC-rich sites characterized by clusters of GCCG, GGCG, GGCA or, more generally, GNCN, and the *Drosophila* Mad consensus sequence (DSC) GCCGC[C/G]G[C/A] found in many Dpp-responding elements (Kim et al., 1997; Xu et al., 1998). We searched also for the Smad-binding element AGAC (SBE or Smad box) (Shi et al., 1998), which is included within the reported Medea consensus site CAGACT (Pyrowolakis et al., 2004). Fragment A, which overlaps with fragments H and K, contains two clusters of GNCNs (referred to as M1 and M2 in Fig. 4B, putative binding sequences in blue). Fragment B, which overlaps with H, K and I, also contains two clusters of GNCNs (M3 and M4). Fragment C, which overlaps with fragment M, contains two notable regions (referred to as M5 and M6 in Fig. 4B), each with a GC-rich region (with a GNCN), an SBE and a DSC. Fragment F contains one GC-rich region (called M7). Oligonucleotides containing these putative Smad sites all formed complexes of varying strengths with GST-Mad protein in mobility shift assays (Fig. 4C). A count of the putative Smad sites yielded between 15 and 20 (Smad-binding sites summarized in Fig. 4E as blue ovals).

The strong binding observed with the M2 and M5 oligonucleotides (Fig. 4C, lanes 6 and 15) could be due to the presence of multiple sites on each oligonucleotide recognized by Mad proteins, which increase the total fraction of probe bound by GST-Mad in the gel shift assay. This also increases the chance of forming multiple band shifts. For example, in Fig. 4C, lane 15, higher order complexes are observed due to the binding of more than one protein molecule to an oligonucleotide. Alternatively, one of the binding sites in the oligonucleotide might have high affinity for GST-Mad and thus contribute to the bulk of the binding. In order to determine if this is the case, M2 and M5 oligonucleotides containing mutations in the Smad recognition sequences were used in mobility shift assays (listed in Fig. 4B, mutations in green). For M2, mutation of GC1, GC2, GC3 and GC4 had variable effects (Fig. 4D, lanes 2-5), with mutation of GC4 reducing binding more significantly than the others (lane 5). However, only when all sites were mutated was M2 binding abolished (lane 6). For M5, it appears that all three sites (GC, SBE and DSC) contribute to Smad binding, although mutation of the GC-rich sequence led to the strongest decrease in binding (lane 8), while mutation of the SBE (lane 9) and each of the half sites of the DSC (ds1 and 2, lanes 10 and 11) had moderate effects. Again, only when all sites were mutated ($M1^m$) was binding completely abolished (lane 12). We can conclude that, although the single

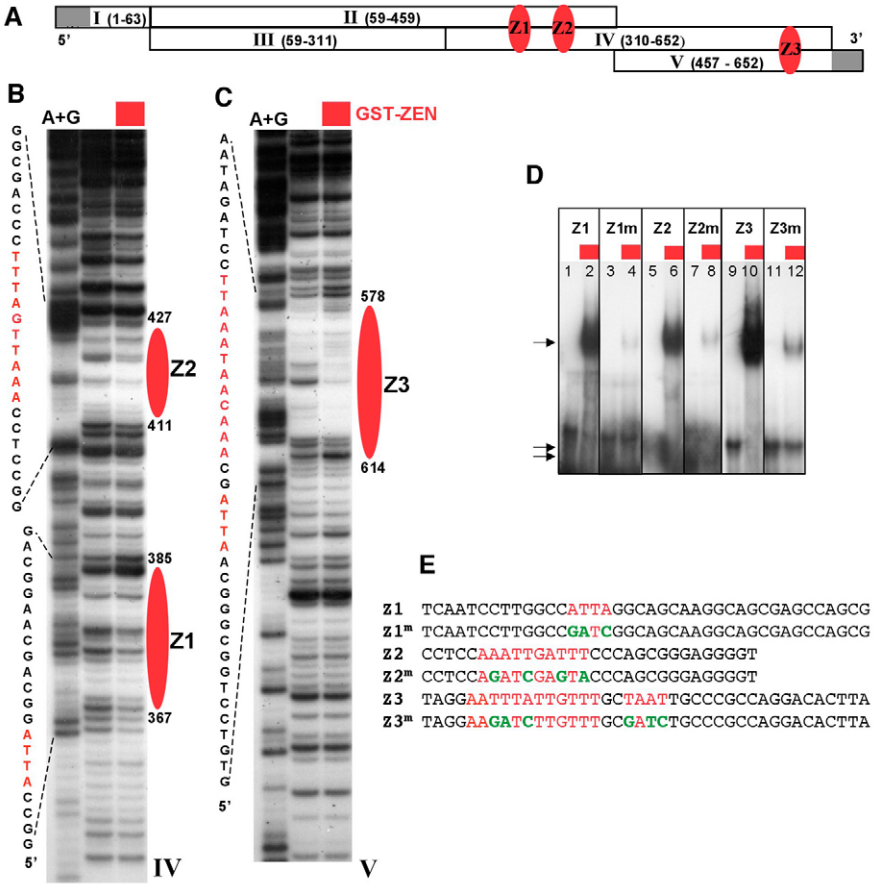

Fig. 3. Zen interacts with the *C15* enhancer. (**A**) Five overlapping fragments comprising the 650 bp enhancer were labeled at one end, incubated with GST-Zen protein, and subjected to DNAse I footprint analysis. Gray boxes at either end represent vector sequences. Only fragments IV (**B**) and V (**C**) displayed footprints. The first lane in each gel represents the chemical degradation of the probe at G+As. The second and third lanes contain fragments that were incubated without or with 60 ng of GST-Zen protein extract (denoted by the red rectangle) prior to DNAse I digestion, respectively. The regions protected by Zen are depicted as red ovals. The nucleotide sequence of the protected regions is shown beside the G+A lanes with putative core binding sites highlighted in red. (**D**) Gel comparing GST-Zen binding to wild-type and mutated oligonucleotides. Arrow, bound probe; two arrows, free probe. (**E**) DNA sequence of wild-type and mutated oligonucleotides used for mobility shift assays and in vitro mutagenesis. Mutations in $Z1^m$, $Z2^m$ and $Z3^m$ are denoted in green.

binding sites in the M2 and M5 clusters contribute differently to the total binding, no one site is essential, and therefore the degree of binding is mostly a result of cumulative action.

We also characterized the putative Smad sites in the M6 and M7 sequences, because, like M5, M6 and M7 are located in the minimal *C15* enhancer (see summary in Fig. 4E). The M6 sequences overlap slightly with the M5 sequence, while the M7 sequences are derived from fragment F at the 3′ end of the 650 bp enhancer. M6, like M5, contains a GC-rich sequence (one GNCN), an SBE and a DSC (Fig. 4B), although M6 produces a much weaker shift compared with M5 (Fig. 4C, lanes 16-18). The M7 sequence contains a GC-rich region (two GNCNs), and like M6 produces a relatively weak shift (Fig. 4C, lanes 19-21). Mutations were introduced into all putative sites all at once in each of the M6 and M7 oligonucleotides (see Fig. 4B) and tested for binding. These mutations abolished binding to GST-Mad (Fig. 4D, lanes 14 and 16).

The results from the DNA-binding assays indicate that there are several clusters of Smad-binding sites in the *C15* 650 bp enhancer (summarized in Fig. 4E, blue ovals). Furthermore, two of the Smad site clusters are in close proximity to two of the Zen sites (red ovals). The M6 oligonucleotide sequence overlaps with the Z1 sequence by seven bases (see Fig. 4E), and the ATTA core site is 20 bases from the DSC in M6. M7 and Z3 completely overlap, and the ATTA core site is immediately adjacent to the GC-rich sequence (see M7 sequence in Fig. 4B). This close proximity of Smad and Zen sites is similar to the situation in the *Race* enhancer, where Zen sites lie on each side of a cluster of Smad sites (Wharton et al., 2004; Xu et al., 2005), although the structure of the two enhancers differs with respect to the number of Smad site clusters and their relative strength of binding. Comparison of the M5 cluster with a 42 bp oligonucleotide (R42 in Fig. 4B) that contains the highest affinity Smad site cluster in the *Race* enhancer (Wharton et al., 2004) showed that the M5 cluster has a much higher binding capability than R42 (Fig. 4C, compare lanes 13-15 with 22-24). Whether high-affinity Smad clusters play a role in activating *C15* in cells with lower levels of Mad-*P* was tested by examining their in vivo relevance in transgenic enhancer-reporter experiments.

The number, rather than the affinity, of Smad sites is important for *C15* expression

As the 650 bp enhancer drives stronger expression than the 350-2 enhancer (Fig. 2D,E), we tested mutant binding site combinations in the context of the *650-lacZ* reporter gene. We focused mostly on the Smad sites in the 350-2 region (M5, M6, M7), as the 350-2 can drive a *C15*-like pattern; however, because the M2 oligonucleotide showed strong binding, it was also tested. We induced mutations in one or more Smad site clusters in the *650-lacZ* transgene identical to those in the $M2^m$, $M5^m$, $M6^m$ and $M7^m$ oligonucleotides that completely abolished DNA binding (Fig. 4D). *lacZ* expression was unaffected in embryos carrying mutations in the M2, M5 or M6 single clusters (Fig. 5A,B, and data not shown, respectively). Embryos carrying a mutation of M7 (Fig. 5C) exhibited reduced levels of expression, with some cells only faintly stained, particularly those at the lateral edges. If these cells are included in the estimate of the number of cells across the domain, then the width is very similar to that of endogenous *C15* (see arrowheads). This reduced expression could be due to the fact that in the M7 sequence there is a Smad site adjacent to a Zen site (Fig. 4E). It is possible that a

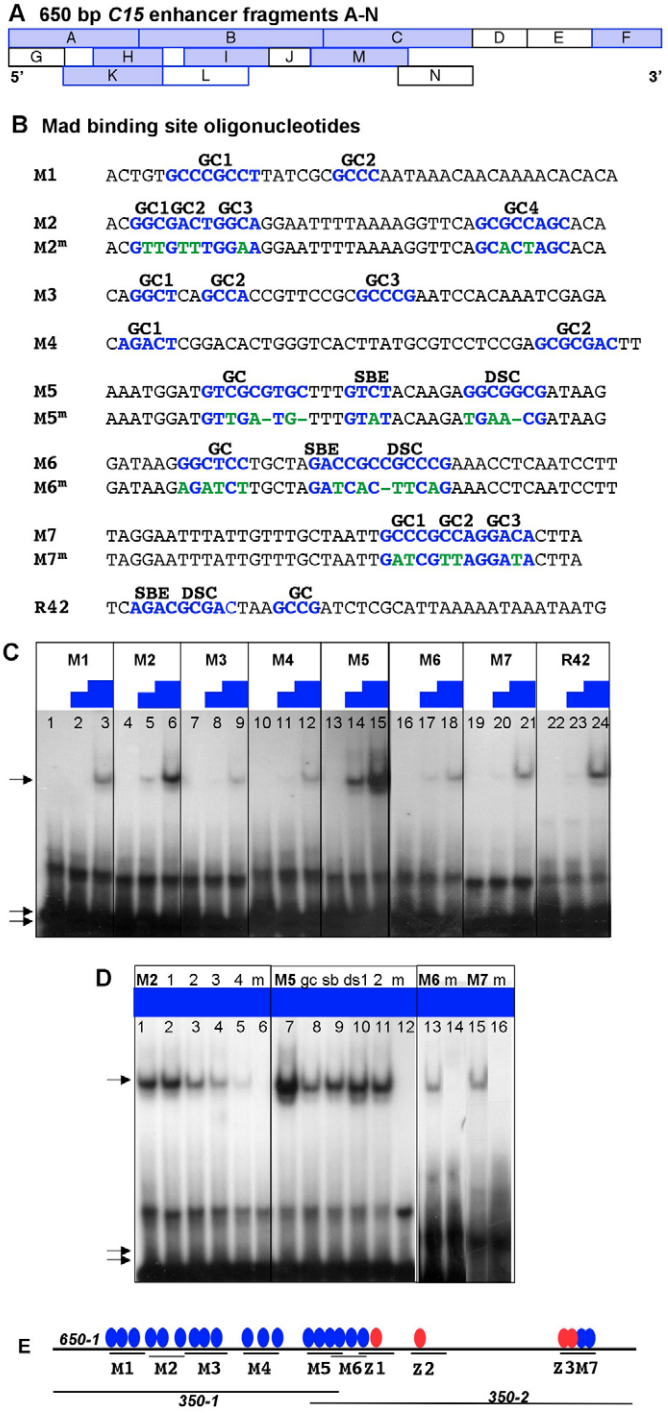

Fig. 4. Smads bind to multiple sites in the *C15* enhancer. (**A**) Schematic representation of the DNA fragments comprising the 650 bp enhancer that were labeled for mobility shift assays with GST-Smad proteins. Fragments that formed complexes are highlighted in blue. (**B**) DNA sequence of wild-type and mutated oligonucleotides containing the putative Smad sites from the *C15* enhancer and one from the *Race* enhancer (R42) that were used for mobility shift assays and in vitro mutagenesis. Putative Smad sites are highlighted in blue, mutated sequences in green. The different types of Smad sites are denoted above the sequences: GC, GC-rich; SBE, Smad-binding element; DSC, *Drosophila* Smad consensus. (**C**) Gel of GST-Mad incubated with the labeled wild-type oligonucleotides. The first lane in each section contains free probe. The second and third lanes contain increasing amounts of GST-Mad (10 and 30 ng; indicated by blue steps). (**D**) Gel of GST-Mad incubated with wild-type (bold) or mutated oligonucleotides. Lanes 1-6, M2 and mutations in one of the four GC-rich sites (denoted 1-4), or all four sites (m). Lanes 7-12, M5 and mutations in the GC (gc), the SBE (sb) or either half of the DSC (ds1, 2), or all of the sites (m). Lanes 13-16, M6, M7 and mutations in all putative sites (m). (**E**) Summary of Smad- (blue ovals) and Zen- (red ovals) binding sites in the 650 bp enhancer (thick black line). Relative locations of the oligonucleotides and the 350 bp enhancers are delineated by thin horizontal lines.

Smad-Zen interaction that facilitates transcriptional activation (Xu et al., 2005) is disrupted in the M7 mutant, and thus expression is reduced compared with wild type.

Double mutant combinations such as M2,5^{m} (Fig. 5D) and M5,7^{m} (Fig. 5E) also led to reduced levels of expression, while others such as M5,6^{m} (data not shown) and the triple mutant M5,6,7^{m} (Fig. 5F) led to a more dramatic reduction in expression. Although the overall domain of expression in these embryos appeared similar to that of endogenous *C15*, the strongest expression was seen close to the midline, where high levels of Mad-*P* and Zen exist. This effect could be the consequence of losing a number of Smad activator sites. Thus, when Smad-binding sites are compromised, low levels of Mad-*P* cannot drive strong expression, whereas high levels of Mad-*P*, found along the midline, can. These results further indicate that Smad sites are important for strength of expression, but do not set the border of expression.

A repression element sets the border of the *C15* expression domain

We also investigated the roles of the Zen-binding sites, which all lie in the 350 bp enhancer (Fig. 4E). We used the Z1^{m}, Z2^{m} and Z3^{m} oligonucleotides that completely abolished DNA binding in each cluster (Fig. 3E) to induce mutations in one or more Zen sites in the *650-lacZ* transgene. Transgenic embryos carrying a mutation in the Z1 site, which contains a canonical ATTA core, showed a reduced level of *lacZ* expression (Fig. 5G). By contrast, mutation of either Z2 or Z3, both of which contain the AT-rich sequence, caused a significant expansion of *lacZ* into the dorsolateral region (Fig. 5H,I), indicating that the Z2 and Z3 sequences mediate repression of *C15* in lateral regions, and in doing so set the border of the *C15* domain. If multiple Zen-binding sites are mutated, overall expression is diminished, presumably because there is less activation in the absence of Zen sites. Mutation of the Z1 and Z2 sites resulted in a similar expansion as in Z2^{m}, but the overall expression was weaker (data not shown), and mutation of all three sites caused a severe reduction of *lacZ* expression (Fig. 5J), indicating that all three sites are important for activation of *C15*. Without activation in these embryos, it is not possible to visualize the lack of repressor function.

We also examined embryos carrying mutations in both the Z2 site and Smad sites. We reasoned that if the expression seen in lateral regions in Z2^{m} embryos is dependent on low levels of Mad-*P*, then abolishing Smad sites might abolish lateral expression. When the M5 cluster of Smad sites was removed in the Z2 background (M5Z2^{m}; Fig. 5K), the same expanded pattern was observed as in Z2^{m} alone, but when two Smad site clusters were removed (M2M5Z2^{m}; Fig. 5L) the pattern narrowed, suggesting that lower levels of the Mad-*P* gradient in lateral regions are insufficient to activate a reporter with compromised Smad sites.

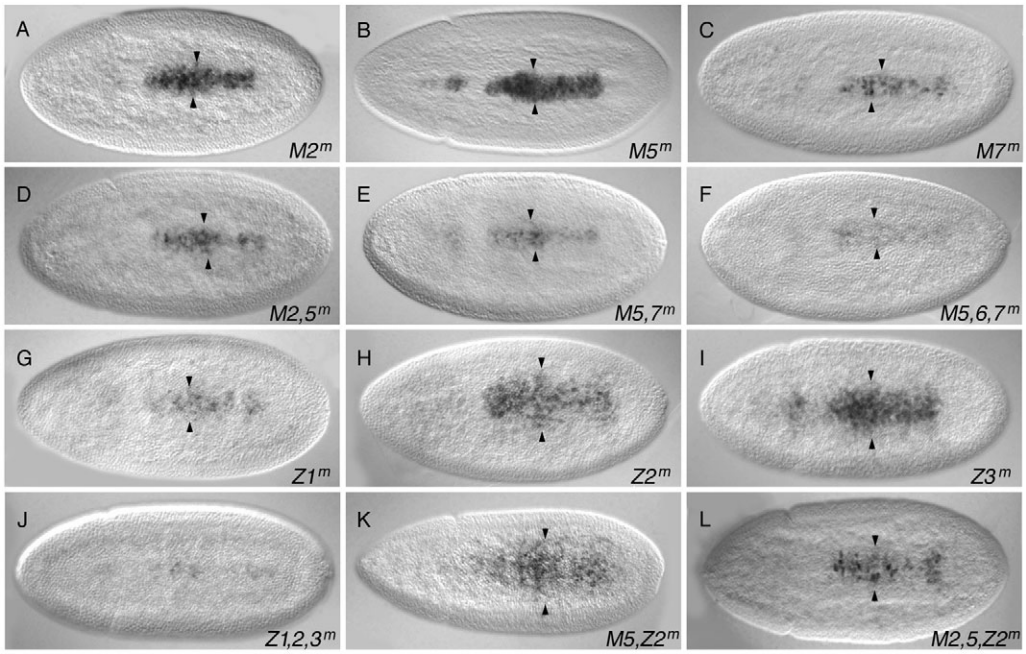

Fig. 5. A combination of the Zen and Smad activators and a repressor are necessary for establishing the *C15* domain. Dorsal views of late stage5/early stage 6 embryos carrying the 650 bp *C15 enhancer-lacZ* transgene with mutations in the Smad- and Zen-binding sites. Embryos were hybridized with *lacZ* probes. Arrowheads indicate the limits of the expression domain. No effect on the *lacZ* expression pattern was observed when Smad sites were mutated in the M2 (**A**) or M5 (**B**) clusters. However, mutation of the Smad sites in M7 (**C**) caused a reduction in the intensity of *lacZ* expression, especially in lateral regions. Arrowheads denote faintly stained cells. Embryos carrying mutations in both the M2 and M5 clusters (**D**) or the M5 and M7 clusters (**E**) also showed weaker *lacZ* expression. Mutation of all Smad sites in M5, M6 and M7 caused severe loss of expression (**F**); however, the overall size of the domain appears unchanged (arrowheads). Mutation of the putative Zen-binding site in the Z1 sequence caused reduced expression (**G**). However, mutation of the Zen sites in the Z2 (**H**) or Z3 (**I**) sequences caused significant expansion of the *lacZ* domain, implicating those sites in repression of the *C15-lacZ* transgene. When the Zen-binding sites were eliminated, expression was drastically reduced (**J**). Mutation of Z2 and M5 had no effect (**K**); however, mutation of M2, M5 and Z2 caused lateral expression to be lost (**L**), presumably because low levels of Mad-*P* in lateral regions is insufficient to activate transcription even in the absence of the putative repressor.

DISCUSSION

Three threshold responses have been described so far for the Dpp morphogen in early *Drosophila* embryos (Jazwinska et al., 1999; Ashe et al., 2000). The Dpp target *C15* has an expression domain with an intermediate width between the Type I gene *Race* and the Type II gene *tup*, yet it can be classified tentatively as a Type II gene because it has the ability to respond to lower than peak levels of Mad-*P* (Fig. 1A,G). Here we investigated the genetic requirements and the enhancer structure of the *C15* gene in order to gain further insight into the mechanisms of its response to the Dpp morphogen. Our results show that three major mechanisms are involved in establishing the unique *C15* domain: (1) combinatorial action of the Dpp signal-transducing Smads and the Zen transcription factor, which is mediated by a genetic feed-forward loop manifested by the dependence of Zen on Dpp, and the requirement of both of them for *C15* activation; (2) an enhancer structure comprising multiple clustered Smad and Zen sites, which ensures enhancer activation in the regions of the embryo with intermediate levels of both transcription factors; and (3) a repression mechanism that prevents *C15* expression in more lateral regions of the embryo, thus setting its expression boundary. As a result, the *C15* enhancer is able to respond to lower threshold levels of Dpp without driving expression as broad as Type II genes.

Mechanisms of *C15* activation

Our genetic experiments show that both Smads and Zen are essential for activation of *C15*. By contrast to *Race*, however, intermediate levels of Smads and Zen can drive *C15* expression (Fig. 1A). Furthermore, the results support the argument that a feed-forward mechanism not only regulates high-level Dpp targets such as *Race* (Xu et al., 2005), but also regulates expression in regions of the embryo where there are intermediate levels of Smads and Zen. This is reminiscent of the regulatory loop established between Dorsal and its target *twist* in the regulation of intermediate-level Dorsal target genes in the neuroectoderm (reviewed by Stathopoulos and Levine, 2002), signifying that common regulatory strategies underlie the response to different morphogens. In experiments in which repression of the *C15* enhancer was abolished, the reporter was expressed in a much broader pattern (Fig. 5H), suggesting that neither Smad nor Zen is limiting for *C15* expression in its normal domain. One can conclude, then, that the Smad/Zen feed-forward loop does not determine the expression limits of *C15*, rather its ability to be activated. And again, this is in contrast to the high-level target *Race*, where Smads/Zen play a direct instructive role in setting the border of expression (Xu et al., 2005). Still, *C15* cannot be expressed in more lateral regions of the embryo where there are lower levels of Smads that allow expression of targets such as *pnr*, even in the presence of large amounts of ectopically expressed Zen (Fig. 1H), so the *C15* enhancer does have its limits in responding to Smads and Zen.

The results of our DNA-binding assays further corroborated the involvement of Smads and Zen in *C15* activation. There are about 15 to 20 Smad sites and three to four Zen sites in the *C15* 650 bp enhancer (Figs 3 and 4). A smaller enhancer of 350 bp (350-2), which contains fewer Smad sites, seven to nine, and all of the Zen

sites (see Fig. 4E), also mediates a normal *C15* pattern, although it is weaker (Fig. 2E). The other small enhancer construct, 350-1, which overlaps with 350-2 by 66 bp, contains plenty of Smad sites (15 to 18), but no Zen sites, and cannot mediate expression, pointing to the importance of the combined activity of Smads and Zen.

Are some of the Smad-binding sites more important for the transcriptional activity of *C15*? In the context of the 650 bp enhancer, removal of either of the high-affinity clusters (M2 or M5) had no effect on reporter expression, and only when additional clusters were also removed was expression lost (Fig. 5F). However, mutation of the M7 cluster reduced reporter expression considerably (Fig. 5C). Although M7 does not show strong binding to Smad proteins, we noticed its close proximity to a Zen binding site. Previously we have shown for the *Race* enhancer that close clustering of Smad- and Zen-binding sites ensures their cooperativity (Xu et al., 2005), suggesting that such effects might be involved in the activation of *C15*. The importance of the clustering of transcription factor-binding sites for their cooperative effect was demonstrated recently for Dorsal and Twist (Zinzen et al., 2006). Similar to the findings reported there, our results support the idea that structural features of the target enhancer, such as the number of modules (binding sites), their close proximity, and the strength of interactions between them, is more important for threshold response than binding affinities.

Setting the expression limits of *C15*

Results from the mutation analysis of the individual Zen-binding sites strongly suggest that a repressor binds to the AT-rich site present in each of the Z2 and Z3 sequences. Embryos carrying the *650-lacZ* transgene with mutated Z2 or Z3 sites show an expanded *lacZ* domain (Fig. 5H,I) suggesting that in the wild-type situation a repressor binds to the AT sites and sets the border of the *C15* domain. What is the repressor? It is not Dorsal or Brinker, because neither binds to AT-rich sites (Ip et al., 1999; Rushlow et al., 2001). Moreover, the dorsoventral (DV) border of *C15* expression is normal in *brk* mutant embryos (M.L., unpublished). It is more likely to be a homeodomain protein that interacts with the AT-rich type of homeodomain-binding site (TCAATTAAAT) (Desplan et al., 1988; Hoey and Levine, 1988). The repressor may be ubiquitously present in the blastoderm embryo or localized to the lateral region. Several new DV genes have been identified in microarray screens for genes differentially expressed along the DV axis, and many of these are expressed broadly in the lateral ectoderm (Stathopoulos et al., 2002; Biemar et al., 2006).

A model for *C15* regulation

Based on our results, we propose the following model for *C15* regulation. *C15* is activated by the combined action of Smads and Zen in the dorsal region of the embryo. The border of the *C15* domain is established by an unknown repressor that binds to the same AT-rich sites to which Zen binds, and competes with Zen for binding. *C15* expression would then depend on a fine balance of the concentration of Smad/Zen activators and the repressor. The threshold response of *C15* that we observed in wild-type and mutant embryos can be accounted for by this model. In the wild-type embryo there is a level of Zen and Smads in the dorsolateral cells, where the repressor is overcome and hence *C15* is expressed. In more lateral cells, the level of Zen is lower, the repressor outcompetes Zen and *C15* is not expressed. In the *sog* mutant embryo, where both Zen and Smads are at medium-high levels in the entire dorsal region (Rushlow et al., 2001), the repressor is outcompeted and *C15* is activated (Fig. 1G). In embryos in which Zen is overexpressed, the repressor is outcompeted and *C15* is activated in lateral regions (Fig. 1H); however, activation is not ubiquitous, strongly suggesting that Zen acts in concert with a certain threshold of Mad-*P* to activate *C15*. These results further support the idea that a particular combined level of Zen and Mad-*P* is required for activation. Below this combined threshold level, *C15* cannot be activated.

One prediction from this model is that it should be possible to manipulate Smad sites such that a change in the border of the *C15* expression domain results. Although none of the Smad site mutant combinations showed a dramatic border change (Fig. 5A-F), we did observe changes when multiple Smad sites were mutated in the Z2 mutant background; i.e. when repressor function was compromised. Elimination of one Smad site cluster in this background had little effect and expression remained broad (Fig. 5K), as expected because mutating one Smad site cluster had no effect before. However, when two Smad site clusters were mutated in the Z2 mutant background, the *C15-lacZ* domain narrowed (Fig. 5L), as if there was now insufficient Smad activity in lateral regions to activate *C15-lacZ*.

Our results demonstrate that the threshold response to the Dpp gradient involves a combinatorial mechanism that includes feed-forward loops and repressor/activator competition. Further studies on additional target genes is required to determine whether any Dpp target genes utilize binding-site affinity as a means to establish threshold responses.

We thank Mu Xu for help with *C15* in situs and Smad gel shifts, and Manfred Frasch for help in identifying putative Smad sites in the *C15* enhancer. We thank Steve Small and Manfred Frasch for many insightful discussions. This study was supported by a grant from the National Institutes of Health, GM63024, and conducted in a facility constructed with support from Research Facilities Improvement Grant C06 RR-15518-01 from the National Center for Research Resources, National Institutes of Health.

References

Ashe, H. L. and Briscoe, J. (2006). The interpretation of morphogen gradients. *Development* **133**, 385-394.
Ashe, H. L., Mannervik, M. and Levine, M. (2000). Dpp signaling thresholds in the dorsal ectoderm of the *Drosophila* embryo. *Development* **127**, 3305-3312.
Biemar, F., Nix, D. A., Piel, J., Peterson, B., Ronshaugen, M., Sementchenko, V., Bell, I., Manak, J. R. and Levine, M. S. (2006). Comprehensive identification of *Drosophila* dorsal-ventral patterning genes using a whole-genome tiling array. *Proc. Natl. Acad. Sci. USA* **103**, 12763-12768.
Campbell, G. (2005). Regulation of gene expression in the distal region of the *Drosophila* leg by the Hox11 homolog, *C15*. *Dev. Biol.* **278**, 607-618.
Dear, T. N. and Rabbitts, H. T. (1994). A *Drosophila melanogaster* homologue of T-cell oncogene HOX11 localises to a cluster of homeobox genes. *Gene* **141**, 225-229.
Desplan, C., Theis, J. and O'Farrell, P. H. (1988). The sequence specificity of homeodomain-DNA interaction. *Cell* **54**, 1081-1090.
Dessain, S. and McGinnis, W. (1993). *Drosophila* homeobox genes. *Adv. Dev. Biochem.* **2**, 1-55.
Dorfman, R. and Shilo, B. Z. (2001). Biphasic activation of the BMP pathway patterns the *Drosophila* embryonic dorsal region. *Development* **128**, 965-972.
Doyle, H. J., Harding, K., Hoey, T. and Levine, M. (1986). Transcripts encoded by a homeobox gene are restricted to dorsal tissues of *Drosophila* embryos. *Nature* **323**, 76-79.
Driever, W., Thoma, G. and Nusslein-Volhard, C. (1989). Determination of spatial domains of zygotic gene expression in the *Drosophila* embryo by the affinity of binding sites for the bicoid morphogen. *Nature* **340**, 363-367.
Ferguson, E. L. and Anderson, K. V. (1992). Decapentaplegic acts as a morphogen to organize dorsal-ventral pattern in the *Drosophila* embryo. *Cell* **71**, 451-461.
Francois, V., Solloway, M., O'Neill, J. W., Emery, J. and Bier, E. (1994). Dorsal-ventral patterning of the *Drosophila* embryo depends on a putative negative growth factor encoded by the short gastrulation gene. *Genes Dev.* **8**, 2602-2616.
Gurdon, J. B. and Bourillot, P. Y. (2001). Morphogen gradient interpretation. *Nature* **413**, 797-803.
Hoey, T. and Levine, M. (1988). Divergent homeo box proteins recognize similar DNA sequences in *Drosophila*. *Nature* **332**, 858-861.
Ip, Y. T., Kraut, R., Levine, M. and Rushlow, C. A. (1999). The dorsal

morphogen is a sequence-specific DNA-binding protein that interacts with a long-range repression element in *Drosophila*. *Cell* **64**, 439-446.
Jagla, K., Bellard, M. and Frasch, M. (2001). A cluster of *Drosophila* homeobox genes involved in mesoderm differentiation programs. *BioEssays* **23**, 125-133.
Jazwinska, A., Rushlow, C. and Roth, S. (1999). The role of *brinker* in mediating the graded response to Dpp in early *Drosophila* embryos. *Development* **126**, 3323-3334.
Jiang, J. and Levine, M. (1993). Binding affinities and cooperative interactions with bHLH activators delimit threshold responses to the dorsal gradient morphogen. *Cell* **72**, 741-752.
Kim, J., Johnson, K., Chen, H., Carroll, S. and Laughon, A. (1997). *Drosophila* Mad binds to DNA and directly mediates activation of vestigial by Decapentaplegic. *Nature* **388**, 304-308.
Kirov, N., Zhelnin, L., Shah, J. and Rushlow, C. (1993). Conversion of a silencer into an enhancer: evidence for a co-repressor in dorsal-mediated repression in *Drosophila*. *EMBO J.* **12**, 3193-3199.
Kissinger, C. R., Liu, B. S., Martin-Blanco, E., Kornberg, T. B. and Pabo, C. O. (1990). Crystal structure of an engrailed homeodomain-DNA complex at 2.8 A resolution: a framework for understanding homeodomain-DNA interactions. *Cell* **63**, 579-590.
Kojima, T., Tsuji. T. and Saigo, K. (2005). A concerted action of a paired-type homoeobox gene, aristaless, and a homolog of Hox11/flx homeobox gene, *clawless*, is essential for the distal tip development of the *Drosophila* leg. *Dev. Biol.* **172**, 434-445.
Lecuit, T., Brook, W., Ng, M., Calleja, M., Sun, H. and Cohen, S. M. (1996). Two distinct mechanisms for long-range patterning *by decapentaplegic* in the *Drosophila* wing. *Nature* **381**, 387-394.
Nellen, D., Burke, R., Struhl, G. and Basler, K. (1996). Direct and long-range action of a Dpp morphogen gradient. *Cell* **85**, 357-368.
Ochoa-Espinosa, A., Yucel, G., Kaplan, L., Pare, A., Pura, N., Oberstein, A., Papatsenko, D. and Small, S. (2005). The role of binding site cluster strength in Bicoid-dependent patterning in *Drosophila*. *Proc. Natl. Acad. Sci. USA* **102**, 4960-4965.
Pyrowolakis, G., Hartmann, B., Müller, B., Basler, K. and Affolter, M. (2004). A simple molecular complex mediates widespread BMP-induced repression during *Drosophila* development. *Dev. Cell.* **7**, 229-240.
Raftery, L. A. and Sutherland, D. J. (2003). Gradients and thresholds: BMP response gradients unveiled in *Drosophila* embryos. *Trends Genet.* **19**, 701-708.
Rushlow, C., Frasch, M., Doyle, H. and Levine, M. (1987). Maternal regulation of zerknullt: a homoeobox gene controlling differentiation of dorsal tissues in *Drosophila*. *Nature* **330**, 583-586.
Rushlow, C., Colosimo, P. F., Lin, M. C., Xu, M. and Kirov, N. (2001). Transcriptional regulation of the *Drosophila* gene *zen* by competing Smad and Brinker inputs. *Genes Dev.* **15**, 340-351.
Shi, Y., Wang, Y. F., Jayaraman, L., Yang, H., Massagué, J. and Pavletich, N. P. (1998). Crystal structure of a Smad MH1 domain bound to DNA: insights on DNA binding in TGF-β signaling. *Cell* **94**, 585-594.
Shimmi, O., Umulis, D., Othmer, H. and O'Connor, M. B. (2005). Facilitated transport of a Dpp/Scw heterodimer by Sog/Tsg leads to robust patterning of the *Drosophila* blastoderm embryo. *Cell* **120**, 873-886.
Stathopoulos, A., Van Drenth, M., Erives, A., Markstein, M. and Levine, M. (2002). Whole-genome analysis of dorsal-ventral patterning in the *Drosophila* embryo. *Cell* **111**, 687-701.
Sutherland, D. J., Li, M., Liu, X. Q., Stefancsik, R. and Raftery, L. A. (2003). Stepwise formation of a SMAD activity gradient during dorsal-ventral patterning of the *Drosophila* embryo. *Development* **130**, 5705-5716.
Tatei, K., Cai, H., Ip, Y. T. and Levine, M. (1995). *Race*: a *Drosophila* homologue of the angiotensin converting enzyme. *Mech. Dev.* **51**, 157-168.
Wang, Y. C. and Ferguson, E. L. (2005). Spatial bistability of Dpp-receptor interactions during *Drosophila* dorsal-ventral patterning. *Nature* **434**, 229-234.
Wharton, K. A., Ray, R. P. and Gelbart, W. M. (1993). An activity gradient of *decapentaplegic* is necessary for the specification of dorsal pattern elements in the *Drosophila* embryo. *Development* **117**, 807-822.
Wharton, S. J., Basu, S. P. and Ashe, H. L. (2004). Smad affinity can direct distinct readouts of the embryonic extracellular Dpp gradient in *Drosophila*. *Curr. Biol.* **14**, 1550-1558.
Wilson, P. A., Lagna, G., Suzuki, A. and Hemmati-Brivanlou, A. (1997). Concentration-dependent patterning of the *Xenopus* ectoderm by BMP4 and its signal transducer Smad1. *Development* **124**, 3177-3184.
Xu, M., Kirov, N. and Rushlow, C. A. (2005). Peak levels of BMP in the *Drosophila* embryo control target genes by a feed-forward mechanism. *Development* **132**, 1637-1647.
Xu, X., Yin, Z., Hudson, J. B., Ferguson, E. L. and Frasch, M. (1998). Smad proteins act in combination with synergistic and antagonistic regulators to target Dpp responses to the *Drosophila* mesoderm. *Genes Dev.* **12**, 2354-2370.
Zinzen, R. P., Senger, K., Levine, M. and Papatsenko, D. (2006). Computational models for neurogenic gene expression in the *Drosophila* embryo. *Curr. Biol.* **16**, 1358-1365.